SWAMP SCIENTIFIC REPORT - GROUP D

Marco Celesti[1], Michal Krupinski[2], Magdalena Smigaj[3] and Dimitris Stratoulias[4]

1. University of Milano-Bicocca, Remote Sensing of Environmental Dynamics Lab., Dept. of Earth and Environmental Sciences, Piazza della Scienza, 1 20126 Milan, Italy; m.celesti2@campus.unimib.it
2. Space Research Centre (CBK PAN), Earth Observation Group, Warsaw, Bartycka 18A, Poland; mkrupinski@cbk.waw.pl
3. School of Civil Engineering and Geosciences, Newcastle University, Newcastle upon Tyne, NE6 5RA, UK; m.smigaj@ncl.ac.uk
4. ITC Faculty of Geo-Information Science and Earth Observation, University of Twente, PO BOX 217, 7500 AE, Enschede, the Netherlands; d.stratoulias@utwente.nl

INTRODUCTION AND AIM OF THE EXPERIMENTS

This report describes the field protocols and instruments used, as well as data collected during the SWAMP training course's field campaign, which took place on the 11th July 2015. The data was collected and analysed by Group D, consisting of the trainees Marco Celesti, Michal Krupinski, Magdalena Smigaj and Dimitris Stratoulias and supervised by Christiaan van der Tol. The collected data relate fluorescence and chlorophyll concentration from 5 different vegetation species encountered in the POLWet site.

The main objectives of this study were to (1) invert the leaf mode of SCOPE (Soil Canopy Observation, Photochemistry and Energy fluxes) model using leaf level measurements, (2) derive biophysical and biochemical parameters, and (3) use these parameters together with Leaf Area Index (LAI) to parameterise SCOPE in forward mode to obtain reflectance, fluorescence, Gross Primary Production (GPP) and Bidirectional Reflectance Distribution Function (BRDF) at canopy level. Moreover, the vegetation canopy's BRDF for one site with the full SCOPE model was simulated, parameterised with results obtained in the first analysis and canopy level LAI measurements, and then compared with BRDF measured from an Unmanned Aerial Vehicle (UAV) at the same site from a partner EUFAR training group (i.e. group E).

Sun-Induced Chlorophyll Fluorescence

Sun-Induced Chlorophyll Fluorescence (SIF) is an electromagnetic radiation emitted by plants during the photosynthetic process in the red and near-infrared regions of the spectrum. It is a relatively weak signal, especially if compared to the amount of radiation absorbed, reflected and transmitted by plants. Nevertheless, it gives the possibility to obtain an indirect and non-intrusive information about the photosynthetic process. Starting from 1970s, the possibility of estimating SIF from Remote Sensing data has been extensively tested, and a number of instruments and retrieval methods has been proposed ([1]).

In recent years, several SIF estimates in the far-red region have been produced at global scale ([2],[3], [4]), and the recently selected FLEX mission from European Space Agency (ESA, Earth-Explorer 8) aims to provide canopy level SIF estimates in both red and far-red region at global scale ([5]). This growing interest emphasises the necessity of developing robust schemes for SIF retrieval at all scales, from leaf to ecosystem. Within this context, the development, testing and validation of models able to simulate SIF at these scales are evidently important.

DESCRIPTION OF THE TEST SITE

The POLWet experimental study site is located near Rzecin, Poland (52º45' N latitude, 16º18' E longitude, 54 m a.s.l., Figure 1), within a mesotrophic peatland. In the middle of the peatland, a thick carpet of peat-substrate overgrown mostly by mosses floats over a free water layer and saturated sediment is encountered. This semi-natural wetland ecosystem is owned by Poznan University of Life Sciences, with the Rzecin measuring station developed and managed by the Agrometeorology Department.

---

[1] Meroni, M., Rossini, M., Guanter, L., Alonso, L., Rascher, U., Colombo, R., & Moreno, J. (2009). Remote sensing of solar-induced chlorophyll fluorescence: Review of methods and applications. *Remote Sensing of Environment*, *113*(10), 2037–2051. http://doi.org/10.1016/j.rse.2009.05.003

[2] Joiner, J., Guanter, L., Lindstrot, R., Voigt, M., Vasilkov, A. P., Middleton, E. M., Huemmrich, K. F., Yoshida, Y. & Frankenberg, C. (2013). Global monitoring of terrestrial chlorophyll fluorescence from moderate-spectral-resolution near-infrared satellite measurements: methodology, simulations, and application to GOME-2. *Atmospheric Measurement Techniques, 6*(10), 28032823. doi:10.5194/amt-6-2803-2013

[3] Guanter, L., Zhang, Y., Jung, M., Joiner, J., Voigt, M., Berry, J. A., Frankenberg, C., Huete, A. R., Zarco-Tejada, P. J., Lee, J. E., Moran, M. S., Ponce-Campos, G., Beer, C., Camps-Valls, G., Buchmann, N., Gianelle, D., Klumpp, K., Cescatti, A., Baker, J. M., & Griffis, T. J. (2014). Global and time-resolved monitoring of crop photosynthesis with chlorophyll fluorescence. *Proceedings of the National Academy of Sciences*, 201320008. doi:10.1073/pnas.1320008111

[4] Frankenberg, C., O'Dell, C., Berry, J., Guanter, L., Joiner, J., Khler, P., Pollock, R. & Taylor, T. E. (2014). Prospects for chlorophyll fluorescence remote sensing from the Orbiting Carbon Observatory-2. *Remote Sensing of Environment, 147,* 112. doi:10.1016/j.rse.2014.02.007

[5] ESA (2015). Report for Mission Selection: FLEX. ESA SP-1330/2 (2 volumes series), Noordwijk, The Netherlands: European Space Agency.

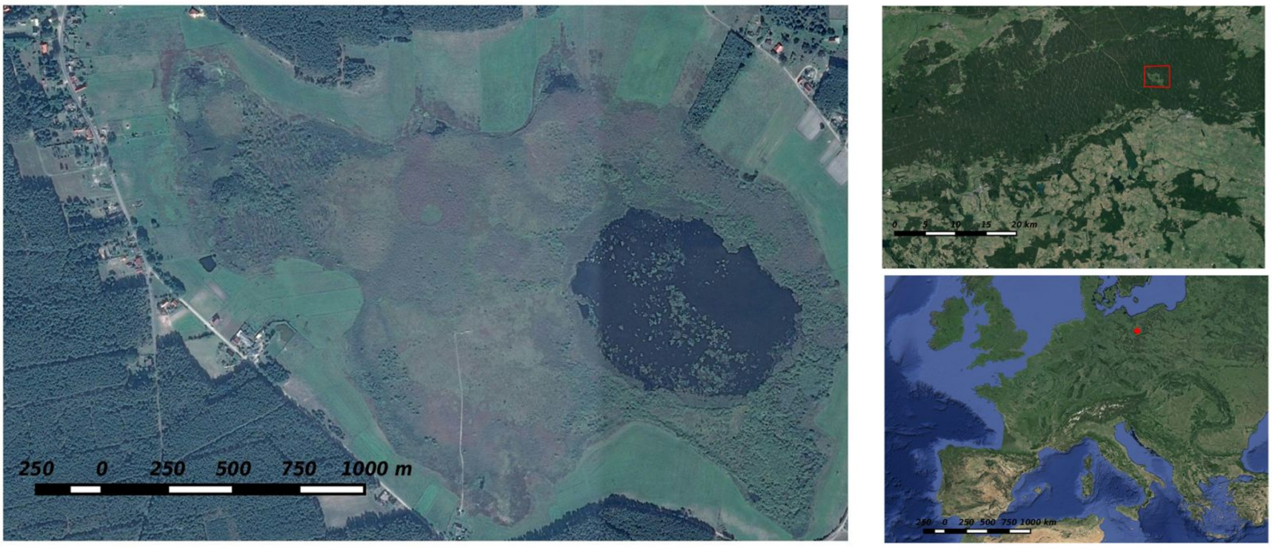

Figure 1: True-colour satellite image of the POLWet peatland (left), and it's location in Europe (insets on the right), © Google & CNES.

Figure 2: Overview of measurement areas: D80 - Carex spp. (top left), D81 - Typha latifolia (top right), D82 – shrub (bottom left), D83 – supposedly Menyanthes trifoliata L., D84 – unidentified species.

The vegetation of the peatland is dominated by *Sphagnum spp.*, *Dicranum spp.*, *Carex spp.*, *Phragmites australis*, *Typha latifolia*, *Oxycoccus palustris Pers.*, *Drosera rotundifolia L.*, *Potentilla palustris L.*, *Ranunculus acris L.* and *Menyanthes trifoliata L.* ([6]). Within this area, two homogeneously vegetated plots were established in order to perform a stratified sampling in canopies of *Carex spp.* (D80), and *Typha latifolia* (D81). Moreover, leaf level measurements of two other unidentified wetland vegetation species (D83 and D84) and a shrub (D82) were performed. Representative images of these sampling areas are presented in Figure 2.

FIELD MEASUREMENTS

The field data collection was undertaken at the POLWET site, Poland on the 11th July 2015 between 6:50 and 14:35 UTC. Measurements were acquired under clear and sunny sky conditions for the most part of the day, except the few last hours of the fieldwork when cirrus clouds appeared; these instances were documented in log sheets. Apart from that, some sporadic clouds appeared throughout day, however care has been taken to avoid measuring when sunlight was blocked by clouds.

The data collection focused on leaf level measurements of five homogeneously vegetated patches (i.e. vegetation targets) identified as D80-D84. For each target, several stable leaves were selected and tagged with a sample ID. In total, 40 sets of measurements were performed for all samples cumulatively. The physical parameters measured in the field were SIF, reflected and transmitted radiance and chlorophyll concentration.

METHODOLOGY

Hyperspectral measurements

Leaf level reflected and transmitted radiance measurements, together with solar incident radiance, were acquired by combining an Ocean Optics USB4000-VIS-NIR spectroradiometer with a FluoWat leaf clip ([7]). The USB4000 characteristics are summarised in Table 1. The FluoWat leaf clip allows measurement of leaf reflected and transmitted radiance, solar incident radiance and, by means of a short-pass filter that blocks the incoming radiation beyond 680 nm, leaf SIF emission spectra (upward and downward).

Table 1: Summary of the USB400-VIS-NIR spectroradiometer's characteristics.

Model	Spect. range [nm]	Nominal FWHM [nm]	N. SSI [nm]	N. SNR
USB4000-VIS-NIR	350-1000	1.5-2.3	0.22	300:1

[6] Juszczak, R., & Augustin, J. (2013). Exchange of the Greenhouse Gases Methane and Nitrous Oxide Between the Atmosphere and a Temperate Peatland in Central Europe. *Wetlands, 33*(5), 895–907. http://doi.org/10.1007/s13157-013-0448-3

[7] Alonso, L., Gomez-Chova, L., Vila-Frances, J., Amoros-Lopez, J., Guanter, L., Calpe, J., & Moreno, J. (2007). Sensitivity analysis of the fraunhofer line discrimination method for the measurement of chlorophyll fluorescence using a field spectroradiometer. *2007 IEEE International Geoscience and Remote Sensing Symposium,3* , 3756–3759. http://doi.org/10.1109/IGARSS.2007.4423660

The USB4000 was cross-calibrated with an ASD FieldSpec Pro the day before the field campaign. A set of measurements for each sample (i.e. each leaf) consisted of 9 consecutive measurements, as per Table 2, and was conducted under stable sunlight conditions. If the solar illumination at ground changed during the measurements of a single set, the procedure was interrupted, documented in the log sheet and repeated. In case of plants with leaves too narrow for successful measurement (i.e. *Carex spp.*), two leaves were joined together to create a viable sample.

The series of measurements on each sample has been set as following. First, a dark current spectrum was recorded at the beginning of each measurement and used to account for the minimum response of the instrument. Then, the filtered and not-filtered incoming radiance over a thin white spectralon panel inserted into the clip were measured, followed by the leaf reflected and transmitted radiance (both filtered and non-filtered). At the end the incident radiance was measured again over the white panel to assure stability of the illumination conditions over the time.

Table 2: Spectrometric measurements conducted sequentially on each sample.

Target	LP Filter	Measurement
Dark target	no	Dark current (DC)
White spectralon	no	Solar incoming radiance
White spectralon	yes	Filtered Solar incoming radiance
Leaf (upper surface)	no	Leaf reflected + emitted radiance
Leaf (upper surface)	yes	Filtered leaf reflected + emitted radiance
Leaf (lower surface)	no	Leaf transmitted + emitted radiance
Leaf (lower surface)	yes	Filtered leaf transmitted + emitted radiance
White spectralon	no	Solar incoming radiance
White spectralon	yes	Filtered Solar incoming radiance

According to this procedure, the following numbers of leaves were sampled: 6 in plot D80, 6 in D81, 4 in D82, 3 in D83, and 4 in D84. In the case of plots D80, D81 and D83, two sets of measurements were undertaken with a time difference of a few hours.

Chl concentration

Chlorophyll concentration in μmol m^{-2} of leaf surface was measured non-destructively with an Apogee MC-100 Chlorophyll concentration meter (Figure 3). The meter measures the ratio of radiation transmittance from red and near infrared wavelengths to internally calculate chlorophyll concentration. Apogee provides custom coefficients for the calculation of chlorophyll concentration in different plants, however none of the sampled species were included. The generic equation (combining all species available in the database) was thus used in this study.

The Chl concentration was converted to mg m^{-2} according to the average Chl molar mass typically encountered in plant leaves (approximately 900 grams per mole) ([8]).

[8] Parry, C., Blonquist, J.M. and Bugbee, B. (2014). In situ measurement of leaf chlorophyll concentration: analysis of the optical/absolute relationship. *Plant, Cell & Environment, 37*(11), 2508-2520.

Figure 3: The Apogee MC-100 Chlorophyll concentration meter, © Apogee.

Modelled data

The Fluspect leaf-level module of the SCOPE model ([9]) version 1.61, was numerically inverted (code by C. Van der Tol and W. Verhoef) using leaf reflectance and transmittance, to retrieve leaf biochemical and biophysical parameters, and automatically run in forward mode to simulate upward and downward leaf SIF spectra. The inversion was performed on a spectral subset of the original data (400-900nm) in order to avoid noisy spectral regions close to the limits of the spectrometer's range.

Data consolidation and processing

Ad hoc R and Matlab scripts have been produced to process the data acquired, in particular:

- **rename_spectra.R** - performing naming manipulation to comply with the SPECCHIO requirements and log file naming convention agreed on prior to the fieldwork;
- **sorting.R** - assigning identifiers to file names and matching them with the samples and clusters. Data sieving was also performed with this script;
- **DN_to_rad.m** - converting data acquired in digital numbers (DN) to physical units (radiance, in $mWm^{-2}sr^{-1}nm^{-1}$). This step is performed using calibration coefficients obtained from spectrometer's calibration;
- **FluoWat_proc.m (and sub-functions Fluowat_param_calc and Fluowat_param_plot)** - processing radiance measurements in order to obtain solar incoming radiance, filter transmittance, leaf reflectance, leaf transmittance, as well as upward and downward SIF spectra;
- **plot_leaf_F.m** - plotting in a comprehensive figure all processing outputs.

Python programming language has also been used for chlorophyll concentration data processing, and production of some of the plots.

---

[9] Van Der Tol, C., Verhoef, W., Timmermans, J., Verhoef, A., & Su, Z. (2009). An integrated model of soil-canopy spectral radiances, photosynthesis, fluorescence, temperature and energy balance. *Biogeosciences, 6*(12), 3109–3129.

The processing scheme can be summarised as follows:

- calibration of each collected spectrum;
- assignment of unique ID to each leaf;
- renaming of each file (i.e. each spectrum) in order to contain leaf and site IDs;
- upload of all spectral data and metadata in SPECCHIO database (including chlorophyll concentration values);
- creation of additional metadata files;
- recursive extraction of leaf spectra from SPECCHIO Matlab Sandbox into arrays;
- DC subtraction and calibration;
- computation of reflectance, transmittance and SIF (up and down);
- Fluspect numerical inversion to retrieve leaf parameters and simulate SIF.

RESULTS

Spectral measurements

The full set of collected spectral measurements was processed in order to obtain leaf reflectance, transmittance, as well as upward and downward SIF spectra. Figure 4 shows an example of the output obtained for a single leaf. In general, there was a good agreement between the first and the second white reference (incoming radiance) measurements. The Relative Root Mean Square Error (RRMSE) between the two white reference spectra of each leaf was computed as a quantitative estimate of this agreement, showing a very low average value of 1.67%.

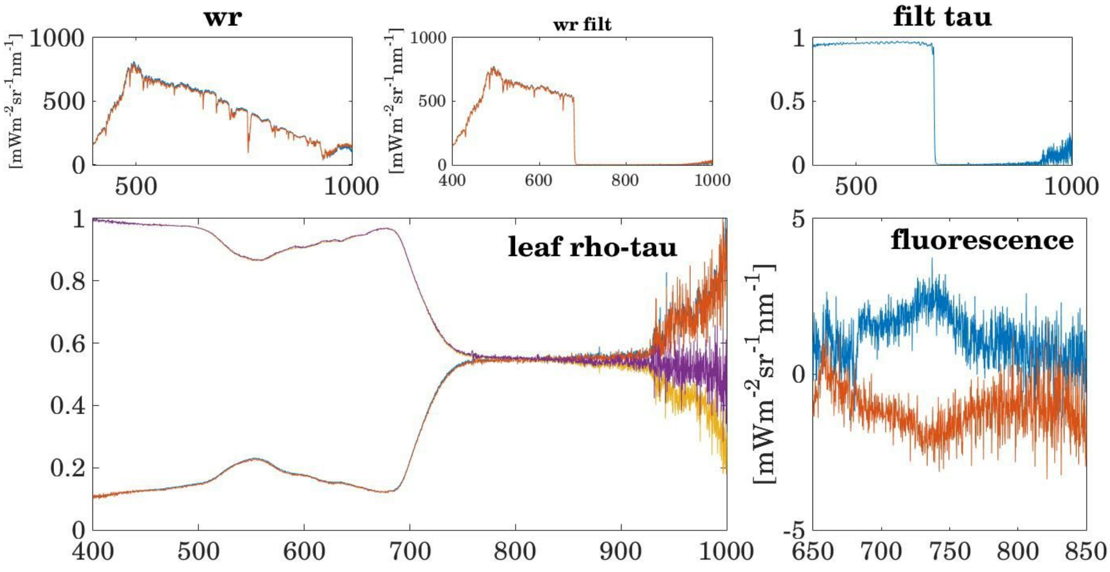

Figure 4: Example spectra from a set of FluoWAT measurements performed on a single leaf of Typha latifolia: solar incoming radiance measured over the white panel (top left), filtered solar incoming radiance (top center), filtered transmittance (top right), leaf reflectance and 1-transmittance (bottom left), upward and downward SIF spectra (bottom right).

Fluorescence values ranged from 0.87 to 4.93 $mWm^{-2}sr^{-1}nm^{-1}$ for SIF measured at 687 nm (SIF peak in the red region), and from 1.80 to 5.73 $mWm^{-2}sr^{-1}nm^{-1}$ for SIF at 740 nm (SIF peak in the far-red region), with extreme values reaching 7.58 and 9.51 $mWm^{-2}sr^{-1}nm^{-1}$, respectively (Figure 5). The peak ratio (SIF740/SIF687) was always positive, with values from 0.95 to 2.84 (Figure 6).

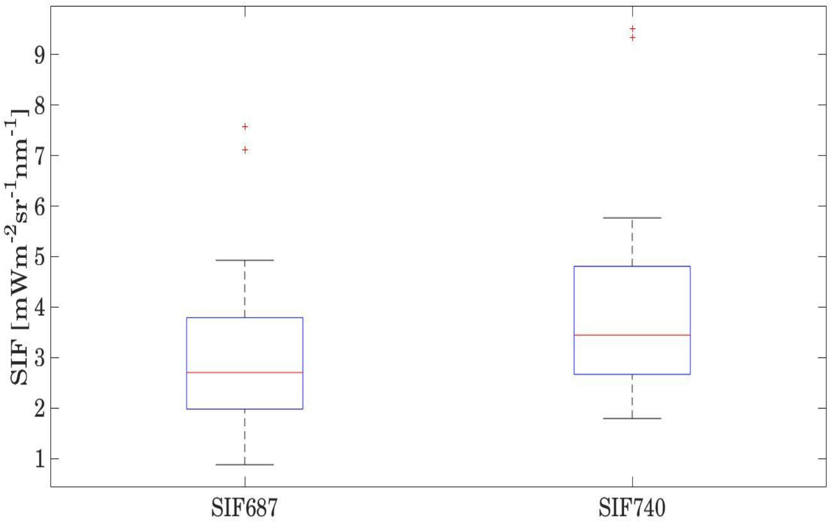

FIgure 5: Boxplot of fluorescence values at 687 nm (SIF peak in the red region) and 740 nm (SIF peak in the far-red region) for all measured leaves.

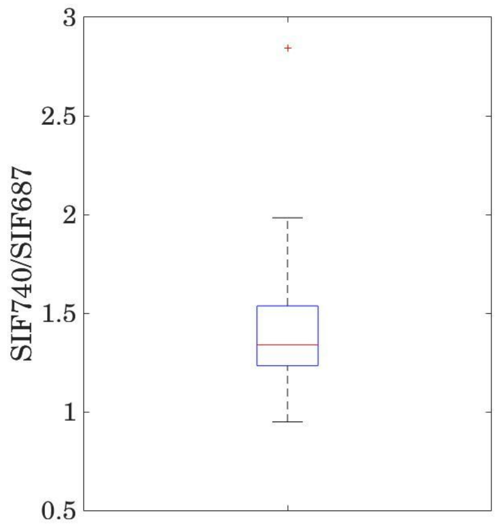

Figure 6: Boxplot of the peak ratio SIF740/SIF687 for all measured leaves.

Figure 7 and Figure 8 show SIF687 and SIF740 values for each measured species. Although *Typha latifolia*'s leaves seem to emit more fluorescence than leaves of other species, they cannot be statistically separated, according to a two-tailed Student's t-test (confidence interval 5%).

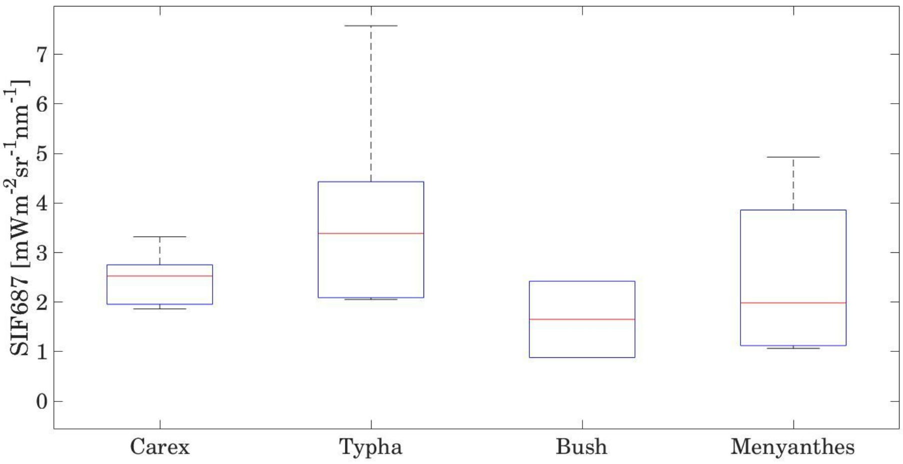

Figure 7: Boxplot of SIF687 values for the measured species.

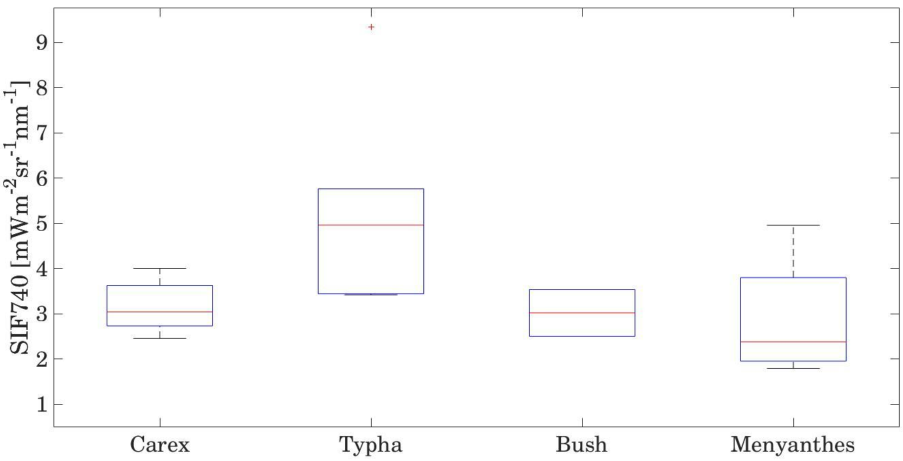

Figure 8: Boxplot of SIF740 values for the measured species.

Chl measurements

Ranges of typical leaf chlorophyll concentrations at sites D80 and D81 were evaluated from multiple measurements, which were performed on randomly chosen leaves of *Carex spp*. and *Typha latifolia*. The corresponding sample sizes were 100 and 162 leaves. In the case of *Carex spp.*, the measurements were performed at the bottom, shaded part of the canopy, as well as at the top, sunlit part (50 measurements for each instance). This procedure was undertaken in order to investigate whether chlorophyll concentrations vary considerably between different parts of the plant. The overlap in histograms and probability density functions (Figure 9) suggests that there is no significant change in chlorophyll concentration distribution across the canopy. Further statistical testing, F test (α = 0.05) and T test (α = 0.05), confirmed that the differences in variance and mean are statistically insignificant, and that the samples can be assumed to come from one population.

The chlorophyll concentration for *Carex spp*. encountered in the field fell within ranges of 88.29 and 399.69 mg m^{-2}, and formed an approximately symmetric sample (skewness of -0.122). The mean value was 252.30 mg m^{-2}, with 68.2% (1σ) and 95.4% (2σ) of values expected to fall within ranges of 193.15-311.45 and 134-370.6 mg m^{-2}.

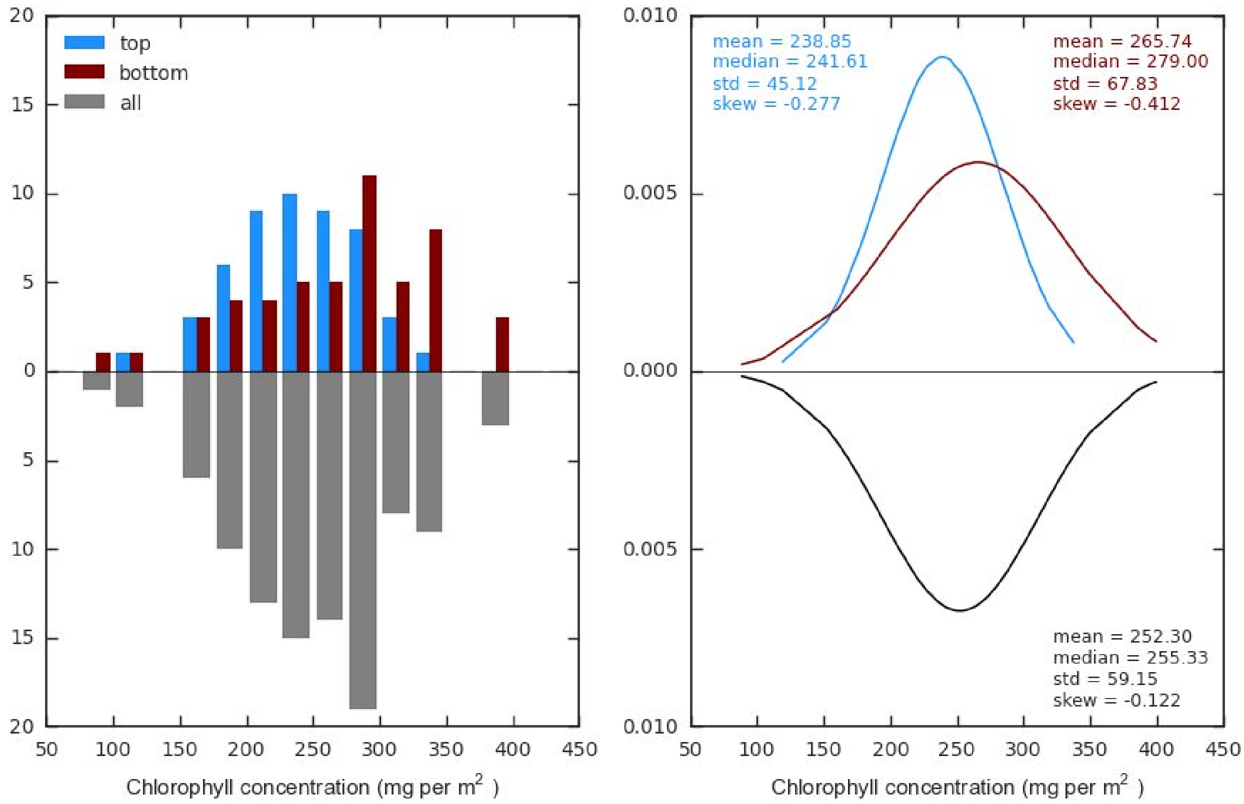

Figure 9: Histograms (left) and probability density functions (right), of Carex spp. chlorophyll concentration samples measured at the top (sunlit) and bottom (shaded) parts of the canopy.

Field values of the chlorophyll concentration measured for *Typha latifolia* ranged from 371.61 to 690.48 mg m^{-2}. The population was marginally right-skewed (skewness of 1.34), with mean and median values of 468.79 and 464.13 mg m^{-2} (Figure 10). The expected ranges for 68.2% (1σ) and 95.4% (2σ) of values to fall within are 421.58-516.00 and 374.37-563.21 mg m^{-2}.

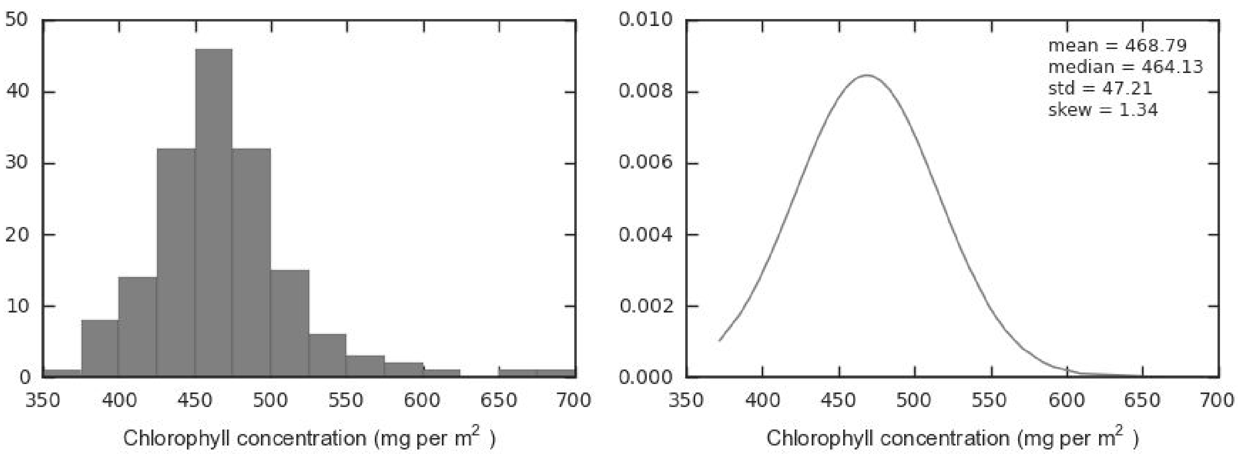

Figure 10: Histogram (left) and probability density function (right) of Typha latifolia chlorophyll concentration sample set.

Chlorophyll concentration values of sample leaves, on which further analysis was based, were averaged from 5 leaf-level measurements. Values of these samples in relation to the whole sets of chlorophyll concentration measurements are presented in Figure 11. The selected leaves form a good representation for both of the plant species, with *Carex spp*. values spreaded above the first quartile, and *Typha latifolia* values located below the fourth quartile.

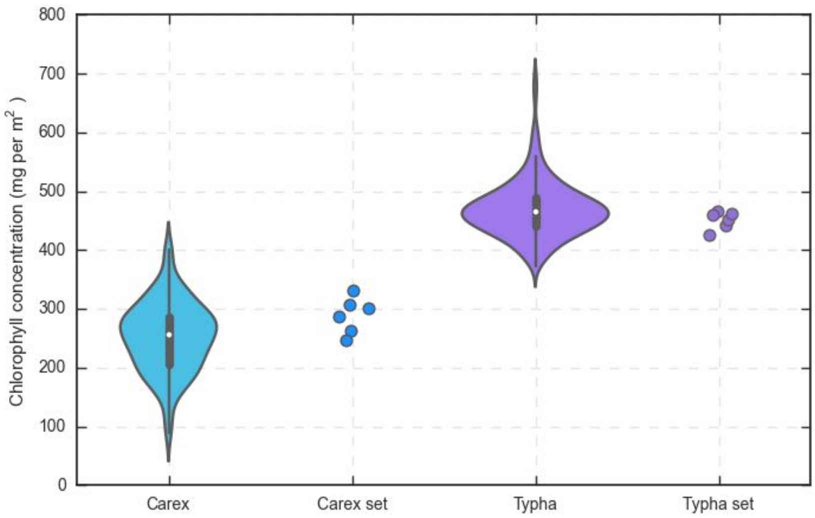

Figure 11: Boxplots with kernel density function plots for Carex spp. and Typha latifolia datasets, along with sets of values used for further analysis.

Inverse modelling

The Fluspect model inversion was run over the entire spectral dataset. Examples of the reflectance and transmittance fitting are presented in Figure 12. In general, there was a good agreement between measured and modelled reflectance and transmittance spectra. Better results were found to be obtained when fitting both spectra combined (instead of reflectance or transmittance data only).

Leaf chlorophyll values retrieved from the model were compared with the observed ones for *Carex spp.* and *Typha latifolia*. The simulated chlorophyll values of *Carex spp.* leaves correlated well with the measured values (Figure 13), unlike in the case of *Typha latifolia* samples (Figure 14). Nevertheless, the retrieved values fell well within the population distribution for both species.

Fluorescence direct modelling presented controversial results; even though in some cases there is a close match between measured and modelled data (Figure 15), it seems that the model generally tends to produce higher SIF687 values than the observed ones (particularly evident when considering *Carex spp.* leaves). Figure 16 shows the boxplots of SIF687 and SIF740 for the four considered species. As already mentioned, SIF687 values are higher than the observed ones, whilst SIF740 values fall closer to the observed ones with relative relationships between species preserved.

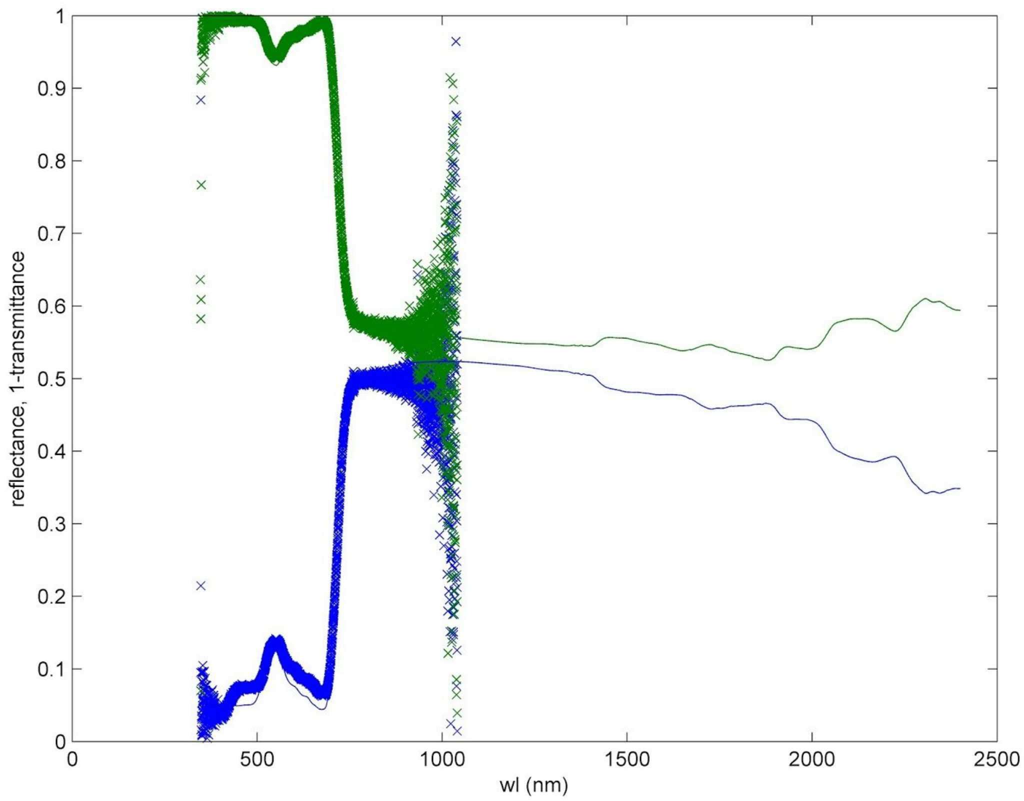

Figure 12: Examples of measured (crosses) and modelled (lines) reflectance (blue) and transmittance (green) spectra.

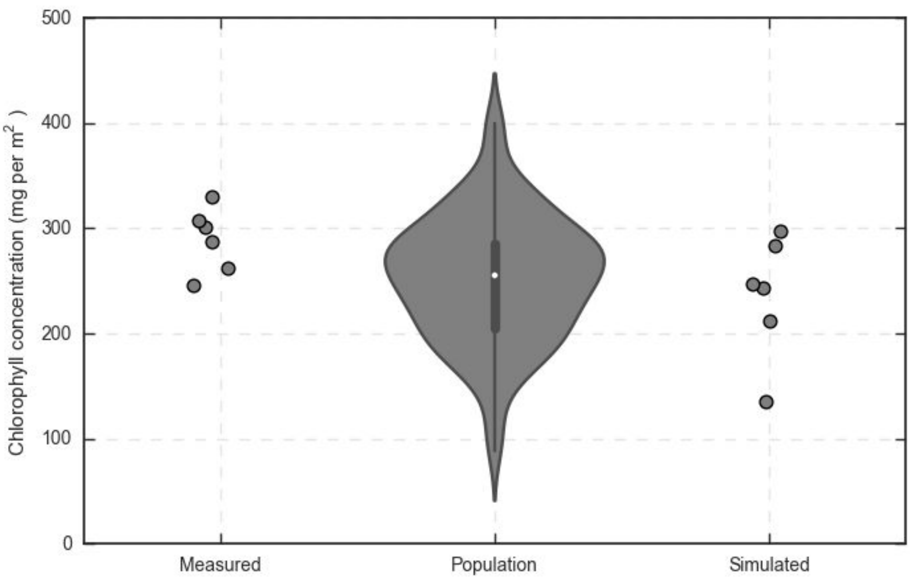

Figure 13: Distribution of chlorophyll values for Carex spp. population, together with measured and simulated (retrieved from the model inversion) values of the sample leaves.

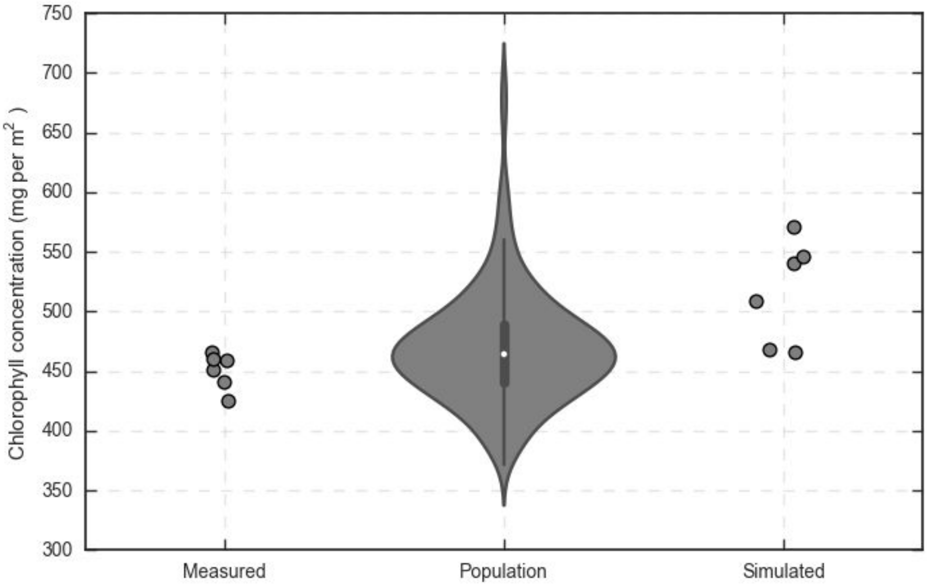

Figure 14: Distribution of chlorophyll values for Typha latifolia population, together with measured and simulated (retrieved from the model inversion) values of the sample leaves.

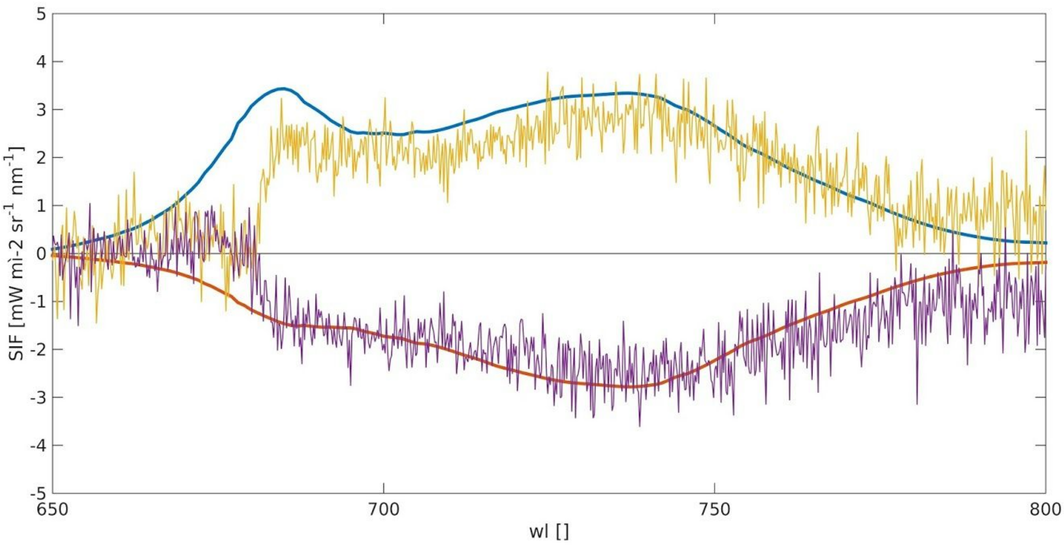

Figure 15: Example of measured and modelled upward and downward SIF spectra with a good agreement between the modelled and observed data.

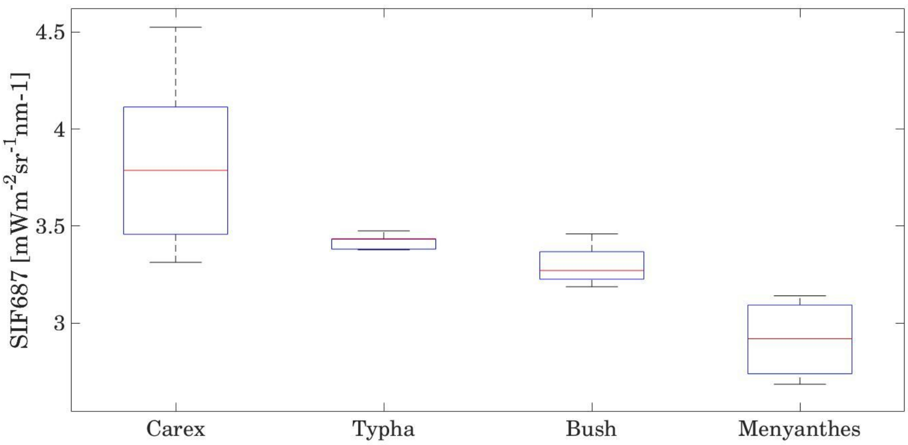

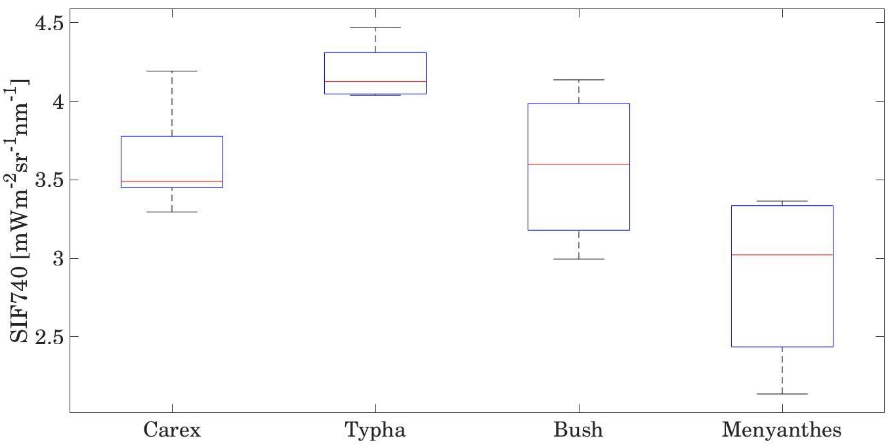

Figure 16: Boxplots of SIF687 (top) and SIF740 (bottom) values for the investigated species.

***BR*DF modelling**

The last part of the project involved comparison of simulated reflectance with reflectance obtained from a UAV-borne spectrometer, providing an opportunity to combine results conducted by three different groups over the same plot. SCOPE model was used to estimate reflectance values (Figure 17) from eight viewing zenith angles (45°E, 33°E, 20°E, 7°E, 6°W, 19°W, 32°W, 44°W). These were compared with the results of in-field UAV-borne measurements made by Group E (Figure 18). The input parameters were exact time of measurements, the same viewing zenith angles and LAI values measured by Group B for *Carex spp.,* as well as leaf biochemical and biophysical parameters obtained from the inversion of the Fluspect model (previous section).

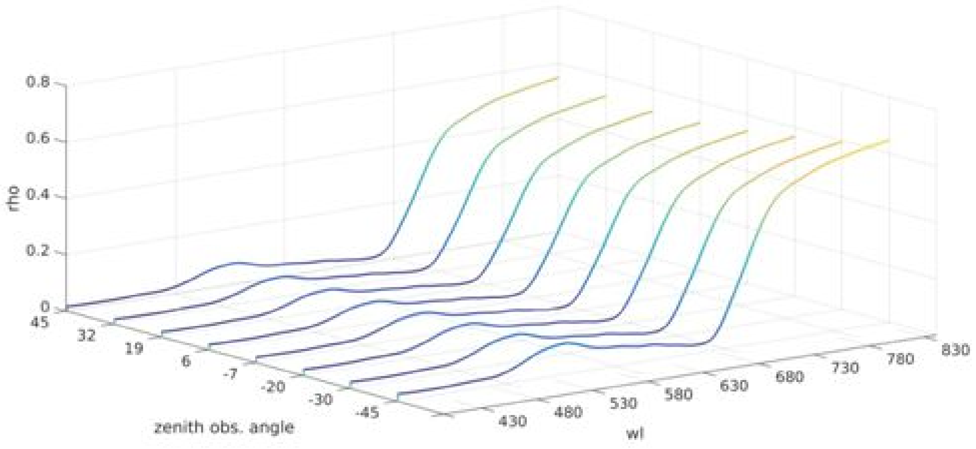

Figure 17: Reflectance values computed with SCOPE model for eight zenith viewing angles.

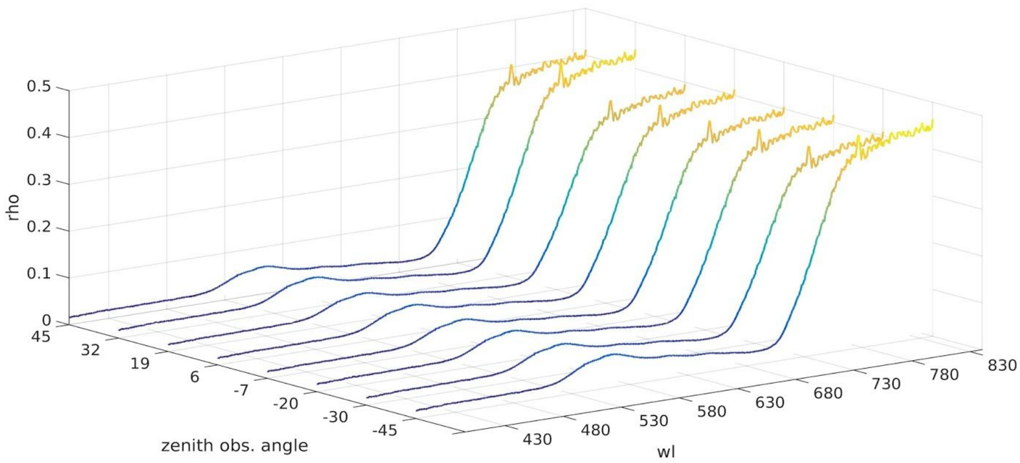

Figure 18: Reflectance values obtained from spectral measurements performed by Group E with UAV platform for eight zenith viewing angles.

We have observed the same shape of modelled and measured spectra with a small shift of values (Table 3). The main difference may be noticed in the near infrared spectral region and exactly after the red-edge where measured values demonstrate noise, a fact that might be attributed to the low sensitivity of the sensor at the longest wavelength of the spectrum measured.

Table 3: Difference between simulated and observed reflectance values (SIM-OBS).

Deg/wvl	430	480	530	580	630	680	730	780	820
45	0.003	0.008	0.039	0.025	0.016	0.002	0.112	0.158	0.180
32	0.002	0.006	0.032	0.019	0.012	0.000	0.102	0.158	0.181
19	0.000	0.004	0.027	0.014	0.008	-0.004	0.078	0.126	0.147
6	0.001	0.004	0.023	0.012	0.007	-0.002	0.067	0.111	0.132
-7	-0.001	0.002	0.016	0.006	0.001	-0.006	0.049	0.089	0.109
-20	-0.002	0.000	0.016	0.005	0.000	-0.008	0.058	0.101	0.121
-30	-0.006	-0.003	0.010	0.001	-0.002	-0.008	0.036	0.065	0.084
-45	-0.004	-0.002	0.016	0.007	0.002	-0.006	0.073	0.111	0.132

CONCLUSIONS

To summarise, this project investigated the use of SCOPE model in forward and inverse modes at leaf and canopy level, based on data collected within the PolWET study area near Rzecin, Poland. The main objectives were to (1) invert the leaf mode of SCOPE model using leaf level measurements, (2) derive biophysical and biochemical parameters, and (3) use these parameters together with LAI to parameterise SCOPE in forward mode to obtain reflectance, fluorescence, GPP and BRDF at canopy level.

Hyperspectral measurements performed at the leaf level showed that fluorescence values of investigated species varied across leaves from 0.87 to 4.93 $mWm^{-2}sr^{-1}nm^{-1}$ for SIF measured at 687 nm, and from 1.80 to 5.73 $mWm^{-2}sr^{-1}nm^{-1}$ for SIF at 740 nm, with extreme values reaching 7.58 and 9.51 $mWm^{-2}sr^{-1}nm^{-1}$, respectively. Nevertheless, differences between species were not statistically significant. It is also worth noting that the peak ratio (SIF740/SIF687) was always positive, with values ranging from 0.95 to 2.84.

At leaf level, higher chlorophyll concentration were observed for *Typha latifolia* samples than for *Carex spp*. (mean value of 468.79 mg m^{-2} in comparison to 252.30 mg m^{-2}). Performed research also showed that in case of *Carex spp*. there is no significant difference in chlorophyll concentration between shaded and non-shaded leaf samples.

The investigation of inverse modelling showed that model generally tends to produce higher SIF687 values than actually measured *in-situ*. It also revealed that modelled chlorophyll concentration in comparison to measurements is lower in case of *Carex spp*. and higher in case of *Typha latifolia*.

Regarding BRDF modelling, reflectance values obtained from UAV platform for eight zenith angles revealed a similarity in shape and generally a shift to longer wavelengths in comparison to the simulated values.

ACKNOWLEDGEMENTS

The research leading to these results has received funding from the European Community's Seventh Framework Programme (FP7/2014-2018) under grant agreement n°312609 (EUFAR: European Facility for Airborne Research in Environmental and Geo-sciences), COST Action ES1309 OPTIMISE (Innovative Optical Tools for Proximal Sensing of Ecophysiological Processes) and the European Space Agency.

REFERENCES

Meroni, M., Rossini, M., Guanter, L., Alonso, L., Rascher, U., Colombo, R., & Moreno, J. (2009). Remote sensing of solar-induced chlorophyll fluorescence: Review of methods and applications. *Remote Sensing of Environment*, *113*(10), 2037–2051. http://doi.org/10.1016/j.rse.2009.05.003

Joiner, J., Guanter, L., Lindstrot, R., Voigt, M., Vasilkov, A. P., Middleton, E. M., Huemmrich, K. F., Yoshida, Y. & Frankenberg, C. (2013). Global monitoring of terrestrial chlorophyll fluorescence from moderate-spectral-resolution near-infrared satellite measurements: methodology, simulations, and application to GOME-2. Atmospheric Measurement Techniques, 6(10), 28032823. doi:10.5194/amt-6-2803-2013

Guanter, L., Zhang, Y., Jung, M., Joiner, J., Voigt, M., Berry, J. A., Frankenberg, C., Huete, A. R., Zarco-Tejada, P. J., Lee, J. E., Moran, M. S., Ponce-Campos, G., Beer, C., Camps-Valls, G., Buchmann, N., Gianelle, D., Klumpp, K., Cescatti, A., Baker, J. M., & Griffis, T. J. (2014). Global and time-resolved monitoring of crop photosynthesis with chlorophyll fluorescence. *Proceedings of the National Academy of Sciences*, 201320008. doi:10.1073/pnas.1320008111

Frankenberg, C., O'Dell, C., Berry, J., Guanter, L., Joiner, J., Khler, P., Pollock, R. & Taylor, T. E. (2014). Prospects for chlorophyll fluorescence remote sensing from the Orbiting Carbon Observatory-2. *Remote Sensing of Environment, 147*, 112. doi:10.1016/j.rse.2014.02.007

Juszczak, R., & Augustin, J. (2013). Exchange of the Greenhouse Gases Methane and Nitrous Oxide Between the Atmosphere and a Temperate Peatland in Central Europe. *Wetlands*, *33*(5), 895–907. http://doi.org/10.1007/s13157-013-0448-3

Alonso, L., Gomez-Chova, L., Vila-Frances, J., Amoros-Lopez, J., Guanter, L., Calpe, J., & Moreno, J. (2007). Sensitivity analysis of the fraunhofer line discrimination method for the measurement of chlorophyll fluorescence using a field spectroradiometer. *2007 IEEE International Geoscience and Remote Sensing Symposium*, *3*, 3756–3759.

Parry, C., Blonquist, J.M. and Bugbee, B. (2014). *In situ* measurement of leaf chlorophyll concentration: analysis of the optical/absolute relationship. *Plant, Cell & Environment, 37*(11), 2508-2520.

Van Der Tol, C., Verhoef, W., Timmermans, J., Verhoef, A., & Su, Z. (2009). An integrated model of soil-canopy spectral radiances, photosynthesis, fluorescence, temperature and energy balance. *Biogeosciences, 6*(12), 3109–3129.